Tikrit Journal of Engineering Sciences

IRAQI Academic Scientific Journals | TJES Tikrit Journal of Engineering Sciences

Article | Tikrit Journal of Engineering Sciences (2026); 33 (1): 2862

Open Access

Impact of Yellow Oil Fly Ash Content and Particle Size on the Mechanical Performance of Sintered Cu-Gr Hybrid Composites

Abdulkader A. Annaz*, Najeeb S. Abtan

Department of Mechanical Engineering, College of Engineering, Tikrit University, Tikrit, Iraq.

Emails:
Abdulkader A. Annaz ✉ | Najeeb S. Abtan ✉

Abstract:

In the present work, copper hybrid composites reinforced with graphite (Gr) and yellow oil fly ash (YOFA) are fabricated by powder metallurgy. Incorporating yellow oil fly ash (YOFA) improves sustainability as well as mechanical and tribological properties, making it a potential green reinforcement. Pure copper powder was mixed with 3% graphite and YOFA at various concentrations, i.e. 0, 3, 6, 9, and 12 vol.%, as well as particle sizes, i.e., <53, 53–80, 80–125, and 125–150 µm. The mechanical and physical properties, i.e., microhardness, radial compressive strength, wear resistance, density, and porosity, were tested. The results showed that as YOFA concentration and particle size increased, density decreased while porosity decreased despite the large particle size. Microhardness increased significantly with YOFA after its initial decrease due to graphite addition. Radial compressive strength reduced due to graphite and declined further with YOFA; however, it improved considerably at 12 vol.% YOFA. Wear tests (5–20 N, 20 min) showed load-dependent wear behavior, and the best performance was achieved at 9 vol.% YOFA with small particles, suggesting higher load-bearing capacity and more stable tribological properties. YOFA was an excellent reinforcement in terms of improving the tribo-mechanical performance of Cu-Gr composites. A full factorial design was employed to maximize the wear test conditions. ANOVA showed that YOFA content, YOFA particle size, and applied stress were the most significant parameters, supporting the experiment's robustness. The best performance was achieved at 9 vol.% YOFA content across all particle sizes and applied loads, minimizing wear loss.

Keywords:

Copper Composites; YOFA; Graphite; Wear Resistance; Hardness; Tribology.

Highlights:

- YOFA was exploited as a reinforcing agent in Cu–graphite composites.
- ANOVA showed that the wear loss was significantly affected by the YOFA content (~50.9%).
- Fine YOFA particles promoted homogeneous distribution and stable tribolayer formation.

Corresponding Author*:

Abdulkader A. Annaz ✉

Department of Mechanical Engineering, College of Engineering, Tikrit University, Tikrit, Iraq.

Article History:

Received:	24 Dec. 2025
Received in revised form:	31 Jan. 2026
Accepted:	03 Mar. 2026
Final Proofreading:	01 Aug. 2026
Available online:	19 Aug. 2026

Citation:

Annaz AA, Abtan NS. **Impact of Yellow Oil Fly Ash Content and Particle Size on the Mechanical Performance of Sintered Cu-Gr Hybrid Composites**. *Tikrit Journal of Engineering Sciences* 2026; **33**(1): 2862.

https://doi.org/10.25130/tjes.33.1.29

© This Is an Open Access Article Under the cc by License. http://creativecommons.org/licenses/by/4.0/

1.INTRODUCTION

Metal-matrix composites (MMCs) are a major class of composites. They are typically made of an alloy or metal matrix, with another component incorporated as a reinforcement or enhancer to achieve a specific desired property. Their main advantage is their ability to improve mechanical and physical properties by selecting the right matrix-to-reinforcement ratio. Thanks to their exceptional performance, the composites produced are also cost-effective [1, 2]. PMT is popular because it can produce complex forms with precise sizes and shapes at high production rates and affordable prices. To overcome these difficulties, PMT offers appropriate processing technology [3-5]. Copper is used in the thermal and electrical industries because of its advantages. These properties include its high melting point, excellent electrical and thermal conductivity, good formability, and remarkable resistance to frictional wear [6, 7]. Its uses include contactors, combustion chamber wall linings, rocket engines, gas turbine nozzles, and more [7, 8]. Its low hardness, poor arc resistance, and inferior corrosion resistance cause significant problems in electrical contacts, particularly those subjected to sliding wear. Copper can be hardened by adding hard ceramic particles or by age-hardening processes to improve corrosion resistance [9, 10]. Graphite particles can also provide lubrication, which is essential for additives in copper-matrix composites. Because of its lamellar structure, graphite reduces the wear rate and friction coefficient of composites by forming a lubricating transport layer on the counter surface [11, 12]. Combining graphite particles with copper yields composites with beneficial properties, including the graphite's superior lubricating nature and low coefficient of thermal expansion [2], [13-15]. Fly ash (FA), a waste material from fuel combustion, has recently attracted attention as a sustainable reinforcement in copper-matrix composites via powder metallurgy. Copper-based composites with FA inclusions have been reported to have improved hardness and wear resistance and good densification through mixing, compaction, and sintering, with minimal processing-induced environmental waste [16]. Recent studies show that increasing FA content improves microstructural homogeneity and matrix reinforcement to a certain degree, but particle agglomeration can then degrade mechanical performance [17]. Other observations also demonstrate that FA particles act as effective obstacles to dislocation movement, resulting in finer microstructures and enhanced tribological characteristics [18]. Consolidating FA and copper composites is advantageous from both engineering and environmental perspectives; it appears to be a suitable approach for developing high-performance sustainable materials. Recently, researchers have increasingly customized copper matrix composites with different reinforcements to improve their mechanical and tribological behavior. Annaz et al. [1] compared Al-graphite and Cu-graphite self-lubricating composites reinforced with nano-Ag (0–4 vol.%) and reported that adding Ag up to 3% enhanced the hardness, tensile strength, and wear resistance, with copper composites outperforming aluminum. Similarly, Zou et al. [19] indicated that adding SiO2 particles, especially Cu-coated, to Cu-graphite composites improved bonding, hardness, and frictional stability, enhancing wear resistance. Dinaharan et al. [20] developed Cu–fly ash composites (0–20 wt.%) via powder metallurgy and reported that 10 wt.% fly ash achieved the best wear resistance and lowest friction, while higher contents increased porosity and promoted abrasive wear. In a related study, Balamurugan et al. [21] fabricated Cu–fly ash composites (2.5–10 wt.%) and demonstrated improved hardness and wear resistance up to ~7.5–10 wt.%. However, severe wear occurred under higher loads and sliding velocities. More recently, Thanga Kasi Rajan et al. [22] investigated Cu–fly ash composites (3–9 wt.%). The authors revealed that increasing fly ash content improved hardness and corrosion resistance in both acidic and seawater environments. However, compressive strength decreased due to boundary slip mechanisms. In this study, Yellow Oil Fly Ash (YOFA) is introduced as a novel reinforcement material for copper–graphite composites. Unlike conventional fly ash, YOFA is a power-plant byproduct produced by burning heavy fuel oil treated with magnesium oxide (MgO) to remove hazardous heavy elements such as vanadium. Removing these hazardous elements prevents corrosion in turbine blades and maintains their operational integrity, resulting in a cleaner, more compatible reinforcement phase. To the best of the authors' knowledge, this is the first time that YOFA has been incorporated into a copper–graphite system, addressing a clear research gap that has not been explored in previous studies. The unique chemical modification and integration of YOFA not only enhance the composites' mechanical performance, corrosion resistance, and thermal stability, but also offer an innovative approach to transforming industrial by-products into sustainable, high-performance materials. This novelty positions the present work as a significant contribution to advancing eco-friendly composite technologies, with direct relevance to the electronics and automotive industries.

2.MATERIALS AND METHODS

2.1.Preparation of Composites

Copper-metal matrix composites were prepared using powder metallurgy technology. Pure copper powder was used as the matrix material reinforced by a constant graphite content of 3 vol.%, as suggested by [19], and varying yellow oil fly ash (YOFA) contents of 0, 3, 6, 9, and 12 vol%, with different grain sizes of <53(YOFA1), 53–80(YOFA2), 80–125(YOFA3), and 125–150 µm(YOFA4). Additionally, the chemical composition of YOFA, as presented in Table 1, was examined by [23]. Table 2 details the hybrid powder composite. Figure 1 shows the FESEM images of the morphology of as-received raw powders. Copper powders were purchased from Co., Ltd., 7/28 Vardaan House, Darya Ganj, New Delhi-110002 (India). Graphite powder was purchased from Riedel-De Haen AG, Germany, and YOFA powder from Al-Qayyarah power station in Nineveh, Iraq. The YOFA powder was dried at 70 °C for 2 hours, then sieved through a fine mesh for 1 hour to separate grain sizes. The graphite powder was dried at 200 °C for 2 hours to remove moisture and other volatile matter. Using a sensitive electronic balance with an accuracy of 0.0001 g, the composite powders were weighed to the required volumetric ratios. The reinforcing powders were mixed with copper powder in a mechanical mixer for 2 hours to manufacture the hybrid composite. The mixture was then cold-pressed in a uniaxial press at a pressure of 500 MPa for 1 minute, as suggested by [1, 19], in a cylindrical mold using a HOYTOM universal testing machine, resulting in the formation of green compressed samples with a height of 6 mm and a diameter of 10 mm. The green compressed samples were sintered in an electric furnace at 900 °C for 2 hours with a heating rate of 5 °C/min, as suggested by [1, 19], in an argon atmosphere with a purity of 99% to avoid contamination and oxidation, and then cooled to room temperature in the furnace.

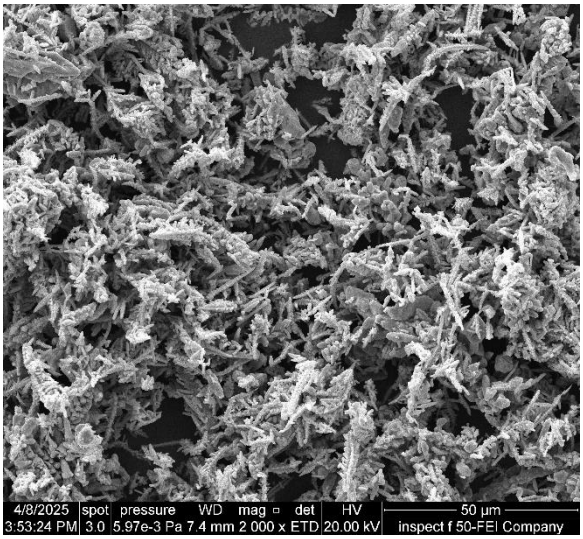
Table 1 Chemical Composition of YOFA [23].

Oxide composition		Elemental composition	
Component	**wt. %**	**Component**	**ppm**
Al_2O_3	0.095	S	302461
Fe_2O_3	2.869	Co	588
CaO	0.488	Cr	3339
MgO	18.761	Cu	25
Na_2O	0.074	Mo	56
TiO_2	0.041	Ni	32905
MnO	0.044	Sr	44
P_2O_5	0.131	V	22626
SO_3	25.5	Zn	507
TOC	7.47	Zr	46
LOI	8.27	La	13
-	-	Pb	21

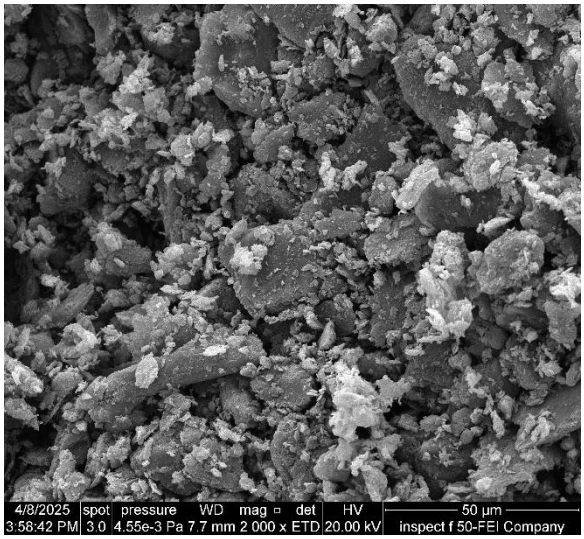
Table 2 Details of Hybrid Composite Powders.

Powder	Particle size	Purity (%)	Shape	Density (g/cm³)	Origin
Cu	≤ 45 µm	99.5	Dendritic	8.94	India
Gr	≤ 63 µm	99.8	Flake	2.26	England
YOFA	< 53 µm 53–80 µm 80–125 µm 125–150 µm	-	Irregular	2.18*	Al Qayyarah Power Plant

(*) YOFA density was measured according to ASTM D2320 (Pycnometer method).



(a)



(b)

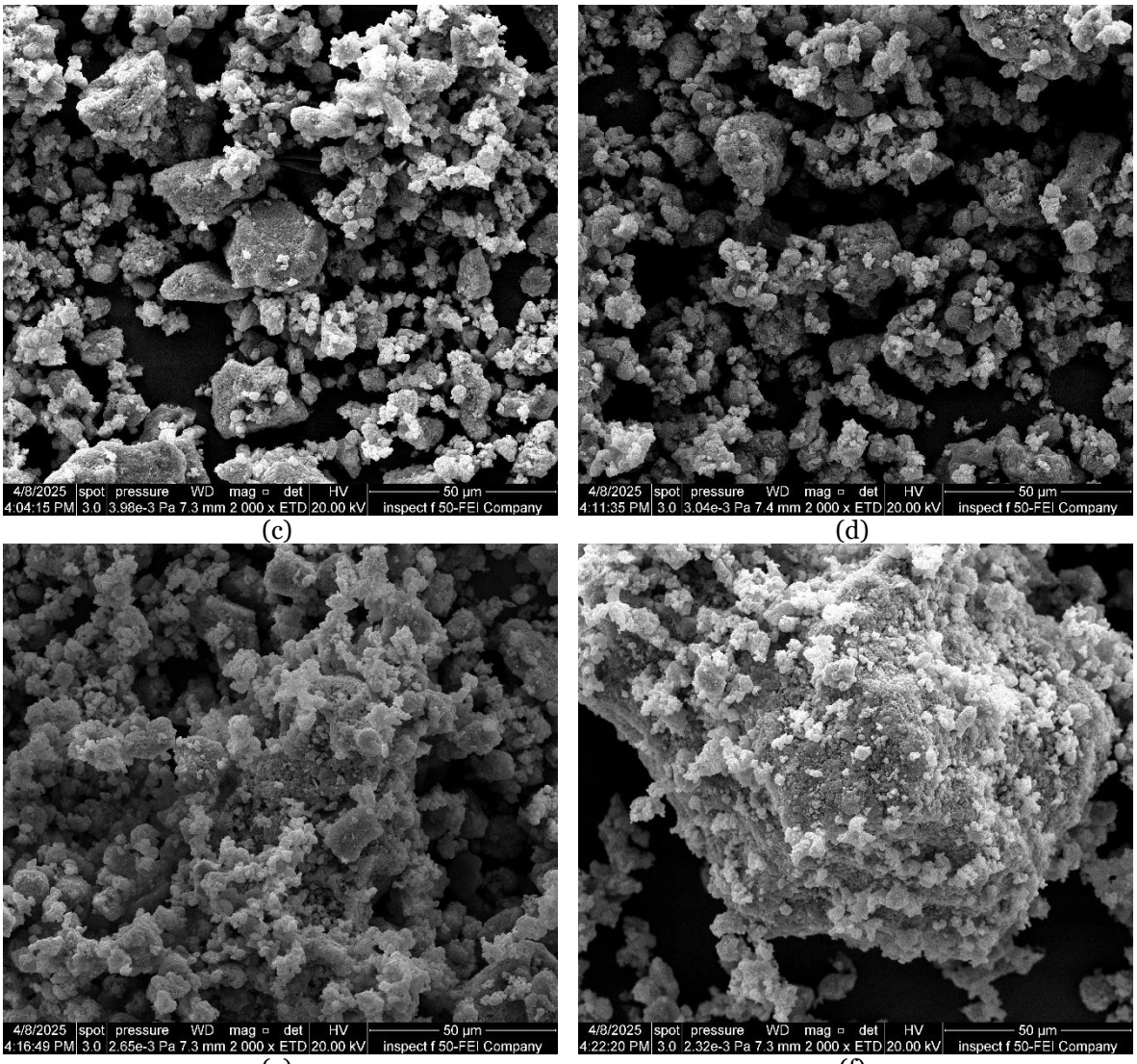


Fig. 1 The FESEM Images of the as-Received Raw Powders: (a) Copper, (b) Graphite, (c) YOFA1, (d) YOFA2, (e) YOFA3, and (f) YOFA4.

2.2.Physical properties

Because they affect material performance, the physical properties of the composite samples were investigated, including density and porosity. Archimedes' principle, as incorporated in the ASTM B962-08 [24], was used to calculate the experimental density. This method determines the sample's mass in air and then infers the volume displaced when the sample is placed in a liquid, usually water. This technique enables precise density determinations, especially for materials with internal voids or micropores. Theoretical density for each sample was calculated from the specific densities of components and their ratios in a mixture using the mixing rule, assuming a homogeneous mixture. The three main materials used were copper, graphite, and (YOFA), with specific densities of 8.94 g/cm³, 2.26 g/cm³, and 2.18 g/cm³, respectively. The theoretical density that can be achieved by this method is a measure for comparison with the experimental density [25]. Porosity (P), the fraction of voids/gaps in a material relative to its total volume, was determined from the theoretical and experimental densities. Since the pore size (and porosity) directly affects the mechanical and thermal properties of bulk material, such as strength, conductivity, and corrosion, to name a few, the pore size is important for the evaluation of sample uniformity, processing influence, and even for the application of predicting within-composite-component distribution. Density and porosity were both accurately determined by using previously validated equations based on the scientific literature and assessed using Eqs. (1), (2), and (3) [26-28].

$$ED = \frac{M_a}{M_a - M_i} \times D_w \qquad (1)$$

where ED, M_a, M_i, and D_w stand for experimental density, sample dry weight, sample weight suspended in distilled water, and water density (Dw=0.997g/cm³ at 25°C), respectively.

$$TD = \sum(TD_i \times X_i) \qquad (2)$$

where TD, TD_i, and X_i are the theoretical density, the theoretical density of the individual composite components, and the volume

fraction of the individual components present in the composite, respectively. Equation (3) expresses porocity.

$$P = (1 - \frac{ED}{TD}) \times 100\% \quad (3)$$

2.3.Mechanical Properties

A study evaluated the mechanical properties and wear behavior of laboratory-prepared hybrid composites. The initial mechanical sample preparation used SiC sandpaper of different grit sizes (1000, 1500, and 2000) to achieve a uniform surface, ultimately followed by fine polishing with a 1 µm Al_2O_3 particle suspension to achieve reliable results. According to ASTM E384-22 [29], the microhardness of the samples was measured using a micro-Vickers hardness tester with a constant load of 10 N for 15 s. To obtain reliable results, a minimum of five readings were averaged for each sample at suitably spaced locations, which allowed an accurate representation of the surface of the sample in terms of resistance to microscopic deformation. Further, the radial compressive strength (DCS) was also investigated. (DCS) is an important mechanical property for hybrid composites because it represents the material's capacity to resist radial loads applied normal to the specimen shape. The test was performed using a Universal Testing Machine (UTM) by applying the load between two flat jaws, following standard procedure. DCS was calculated using Eq. (4) [3], [30-32], which is a function of the load force (N), the specimen thickness (K), and the specimen diameter (L).

$$DSC = \frac{2N}{\pi KL} \quad (4)$$

To evaluate the abrasion resistance, a dry sliding wear test was conducted following ASTM G99-95 [33] using a pin-on-disc tribometer (ED-201, Ducom). The 10 mm diameter and 6 mm thick specimens were assembled in a holder against a hardened steel disc (62 HRC), with the operating parameters fixed at a wear track diameter of 60 mm and a rotating speed of 480 rpm. The test was performed for 20 min at four vertical load levels: 5, 10, 15, and 20 N. Before and after each test, both samples and discs were wiped with acetone to avoid surface contamination affecting the results. Wear loss was calculated from the mass loss of the specimen before and after each test, as described in applicable technical references [2, 31, 32, 34]. Lastly, the topography and morphology of wear traces and worn surfaces were analyzed using a scanning electron microscope (SEM), providing insight into the dominant wear processes and the types of residual surface formations following testing. A flowchart outlining the entire experimental procedure for preparing and evaluating the composite specimens are depicted in Figure 2, providing the reader with a concise step-by-step guide to what is involved.

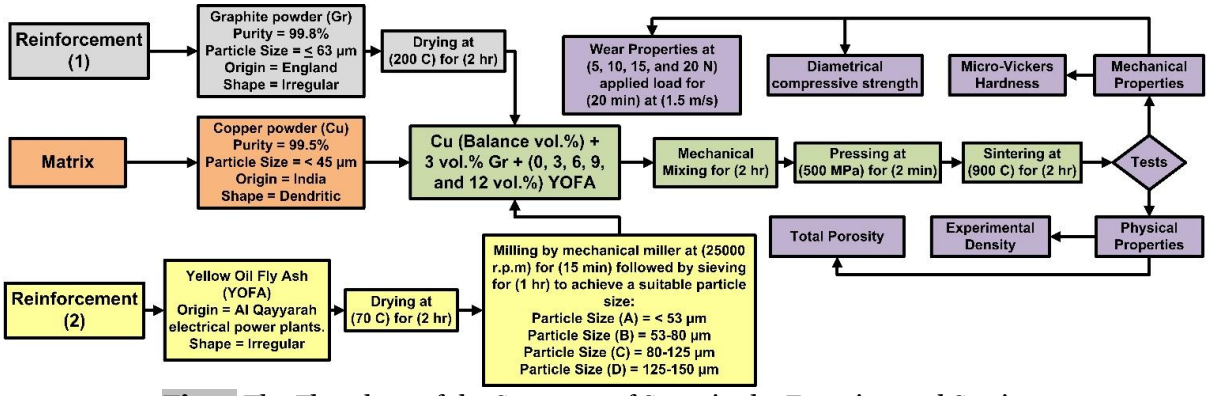


Fig. 2 The Flowchart of the Sequence of Steps in the Experimental Section.

2.4.Design of Experiment Method

Tribo-pairs and contact conditions influence dry sliding wear. Therefore, it is important to understand how each parameter affects wear and how they interact in the abrasive wear of composites. One practical strategy for streamlining intricate testing processes is the Design of Experiments (DOE) method. By considering multiple criteria, it assists in determining the optimal levels of key parameters. Because it allows calculation of overall interactions and the primary impacts of multiple test factors, full-factorial design (FFD) is a crucial component of DOE. Every parameter setting appears alongside every other one in an FFD analysis [35-37]. FFD integrates statistical and mathematical techniques to model and analyze situations in which several variables affect and improve a response. In factorial studies, it is often unclear how the response relates to the independent variables. Thus, estimating the functional relationship between the response (y) and a set of independent variables is a step in factorial design.

1- The experimental trials have been designed using an FFD in accordance with the protocol. To ensure error-free calculations, statistical software such as MINITAB 21 and MS Excel was used, and the results were thoroughly cross-checked.

2- To investigate the tribological behavior of the composites, an FFD analysis was performed. The components that affect the dry sliding wear process must be identified to comprehend it. To describe the samples' wear characteristics, three criteria were selected: YOFA composition, YOFA particle size, and applied normal load. These elements are crucial variables in wear tests that impact the composites' performance. The proper levels of these elements, listed in Table 3, were determined by consulting experts and the literature. The response variable—the copper composites' wear loss — should also be noted. The removal of debris from the contact was successfully controlled by keeping the sliding velocity at a steady 1.5 m/s. As a result, a L96 standard orthogonal array was utilized together with a general FFD. As indicated in Table 4, this array's 96 rows and three columns offer 95 degrees of freedom for adjusting three parameters at various levels. To assess wear, 96 experiments were conducted using various combinations of the three parameters: one extrinsic and two intrinsic, allocated to rows and columns, respectively.

3- The FFD method evaluated Analysis of Variance (ANOVA) to improve control parameters and determine their significance in the dry sliding wear process. The ANOVA tool can serve as a cross-check to verify the importance of input control parameters. ANOVA helps calculate parameter contribution percentages and estimate error variance. Its main aims are to optimize the output response and perform statistical analysis.

Table 3 The Different Factor Levels Used in a Full-Factorial Experimental Design.

No.	Factors / Parameters	Levels					
		1	2	3	4	5	6
1	A: YOFA content (vol.%)	-1*	0	3	6	9	12
2	B: Particle Size of YOFA (µm)	A	B	C	D	-	-
3	C: Applied Normal Load (N)	5	10	15	20	-	-

*(-1 = pure copper)

Table 4 Results of Hybrid Composites' Wear Loss from the FFD Experiment.

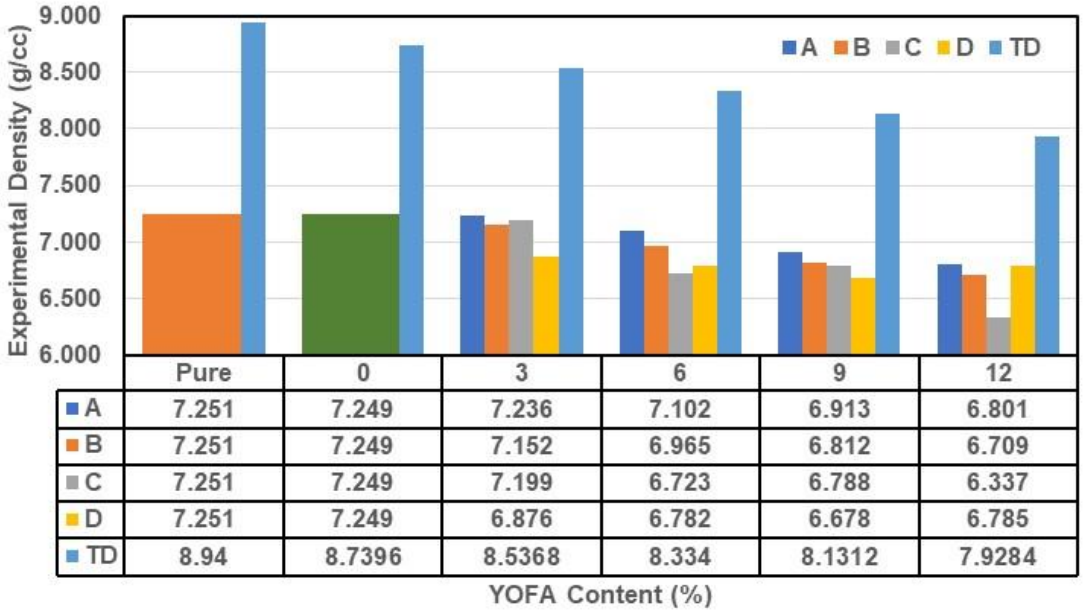
No.	YOFA Content	Applied Load	Particle Size	Wear Loss (g)	No.	YOFA Content	Applied Load	Particle Size	Wear Loss (g)
1	Pure	5	A	0.0144	49	YC6	5	A	0.0074
2	Pure	5	B	0.0144	50	YC6	5	B	0.0005
3	Pure	5	C	0.0144	51	YC6	5	C	0.2439
4	Pure	5	D	0.0144	52	YC6	5	D	1.4994
5	Pure	10	A	0.0181	53	YC6	10	A	0.7853
6	Pure	10	B	0.0181	54	YC6	10	B	2.0008
7	Pure	10	C	0.0181	55	YC6	10	C	0.8488
8	Pure	10	D	0.0181	56	YC6	10	D	2.3251
9	Pure	15	A	0.0198	57	YC6	15	A	0.8738
10	Pure	15	B	0.0198	58	YC6	15	B	2.0382
11	Pure	15	C	0.0198	59	YC6	15	C	1.3292
12	Pure	15	D	0.0198	60	YC6	15	D	2.3137
13	Pure	20	A	0.0265	61	YC6	20	A	2.3028
14	Pure	20	B	0.0265	62	YC6	20	B	2.1059
15	Pure	20	C	0.0265	63	YC6	20	C	2.3143
16	Pure	20	D	0.0265	64	YC6	20	D	2.673
17	YC0	5	A	0.0485	65	YC9	5	A	0.0028
18	YC0	5	B	0.0485	66	YC9	5	B	0.0014
19	YC0	5	C	0.0485	67	YC9	5	C	0.0012
20	YC0	5	D	0.0485	68	YC9	5	D	0.0019
21	YC0	10	A	0.3195	69	YC9	10	A	0.0031
22	YC0	10	B	0.3195	70	YC9	10	B	0.002
23	YC0	10	C	0.3195	71	YC9	10	C	0.0014
24	YC0	10	D	0.3195	72	YC9	10	D	0.0294
25	YC0	15	A	0.335	73	YC9	15	A	0.0034
26	YC0	15	B	0.335	74	YC9	15	B	0.0061
27	YC0	15	C	0.335	75	YC9	15	C	0.0094
28	YC0	15	D	0.335	76	YC9	15	D	0.0326
29	YC0	20	A	0.542	77	YC9	20	A	0.0115
30	YC0	20	B	0.542	78	YC9	20	B	0.0328
31	YC0	20	C	0.542	79	YC9	20	C	0.2657
32	YC0	20	D	0.542	80	YC9	20	D	0.8488
33	YC3	5	A	0.0009	81	YC12	5	A	0.5699
34	YC3	5	B	0.0065	82	YC12	5	B	0.6163
35	YC3	5	C	0.3331	83	YC12	5	C	0.7257
36	YC3	5	D	0.2566	84	YC12	5	D	0.5472
37	YC3	10	A	0.0029	85	YC12	10	A	2.1229
38	YC3	10	B	0.1856	86	YC12	10	B	2.1304
39	YC3	10	C	0.8887	87	YC12	10	C	1.0372
40	YC3	10	D	1.234	88	YC12	10	D	0.6152
41	YC3	15	A	0.0041	89	YC12	15	A	2.0646
42	YC3	15	B	0.0065	90	YC12	15	B	2.3124

43	YC3	15	C	1.3187	91	YC12	15	C	1.3106
44	YC3	15	D	2.4605	92	YC12	15	D	0.7119
45	YC3	20	A	0.5007	93	YC12	20	A	2.1632
46	YC3	20	B	1.3738	94	YC12	20	B	2.4408
47	YC3	20	C	1.6819	95	YC12	20	C	2.0959
48	YC3	20	D	2.5014	96	YC12	20	D	1.3579

3.RESULTS AND DISCUSSION

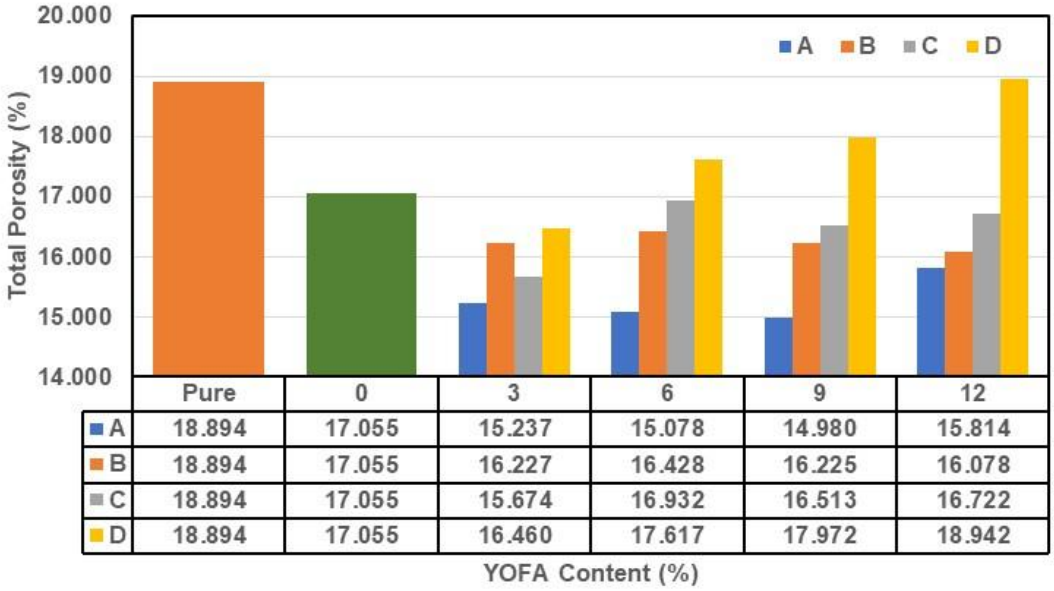
3.1.Density and Porosity

Figures 3 and 4 depict the influence of YOFA content and particle size on the composite material's experimental density and porosity. A clear pattern shows that increasing YOFA content progressively reduced both the experimental and theoretical densities. This phenomenon is attributed to the considerable density disparity between the base metal matrix and the YOFA particles, with the base material possessing around four times the density of the additive. Therefore, when a lighter component such as YOFA is introduced, the denser base material is displaced, reducing the overall composite density [21]. The void ratios of the samples, shown in Figure 4, suggest a more complex pattern. All the YOFA-based samples have lower porosity than the neat (unreinforced) ones. This improvement is most pronounced at smaller particle sizes, likely because they fill the interstices between metal matrix particles better, increasing packing efficiency and reducing porosity. However, porosity tends to increase with YOFA particle size because larger particles penetrate less effectively, disrupting particle packing and forming pores. In addition, an increase in porosity is observed with the increase in YOFA content, particularly at larger particle sizes. This behavior can be explained by the higher likelihood of particle agglomeration at higher YOFA concentrations. These agglomerates act as diffusion barriers during pressing and sintering, preventing homogeneous particle distribution and forming isolated pores [20, 38]. These pores decrease density while increasing the composite's total porosity. Free density and porosity may be maximized by using finer YOFA particles at the lowest concentration. Larger particle sizes and higher YOFA concentrations yield less efficient results because of agglomeration and poor particle packing. It should also be mentioned that a concurrent decrease in the bulk density and porosity was found with increasing content of YOFA. While ceramic reinforcements generally increase porosity and are difficult to densify because of poor wettability, the decrease in porosity in the present study can be explained mainly by the filling of interstitial voids with both fine YOFA and Cu particles. In this work, the fine YOFA particles efficiently filled the interstitial spaces and voids among the larger Cu matrix particles, improving geometric packing efficiency. However, the bulk density decreases, due to the Rule of Mixture, because of the large density difference between the dense copper matrix (8.94 g/cm³) and the low-density YOFA reinforcement (2.18 g/cm³). Therefore, adding YOFA produced a composite that is both lighter and more closely packed.



	Pure	0	3	6	9	12
A	7.251	7.249	7.236	7.102	6.913	6.801
B	7.251	7.249	7.152	6.965	6.812	6.709
C	7.251	7.249	7.199	6.723	6.788	6.337
D	7.251	7.249	6.876	6.782	6.678	6.785
TD	8.94	8.7396	8.5368	8.334	8.1312	7.9284

Fig. 3 Variation of Measured Experimental Density with YOFA Content.

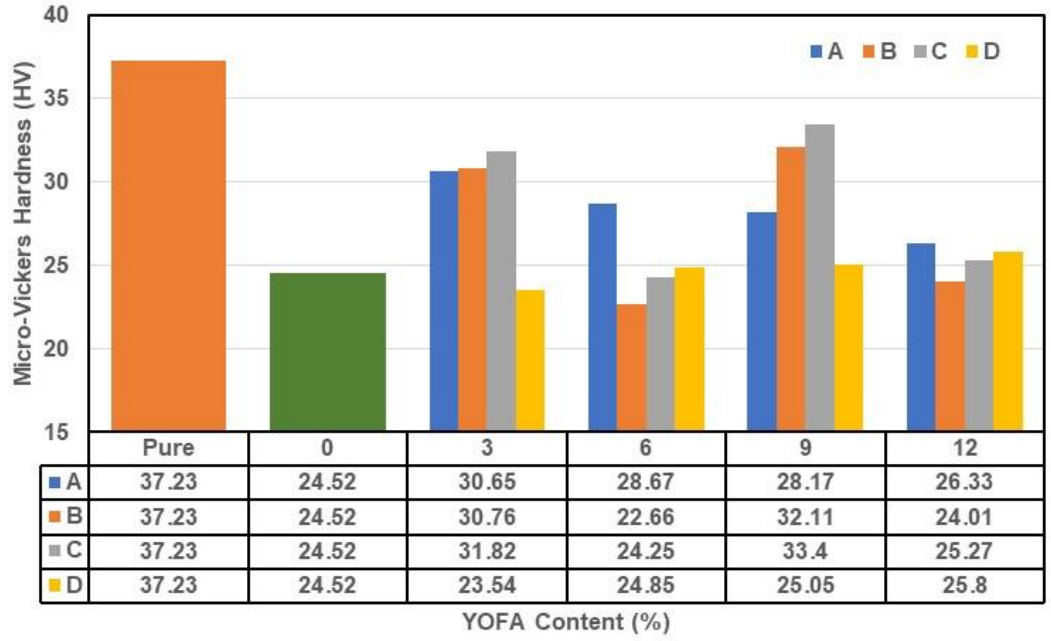


	Pure	0	3	6	9	12
A	18.894	17.055	15.237	15.078	14.980	15.814
B	18.894	17.055	16.227	16.428	16.225	16.078
C	18.894	17.055	15.674	16.932	16.513	16.722
D	18.894	17.055	16.460	17.617	17.972	18.942

Fig. 4 Variation of Measured Total Porosity with YOFA Content.

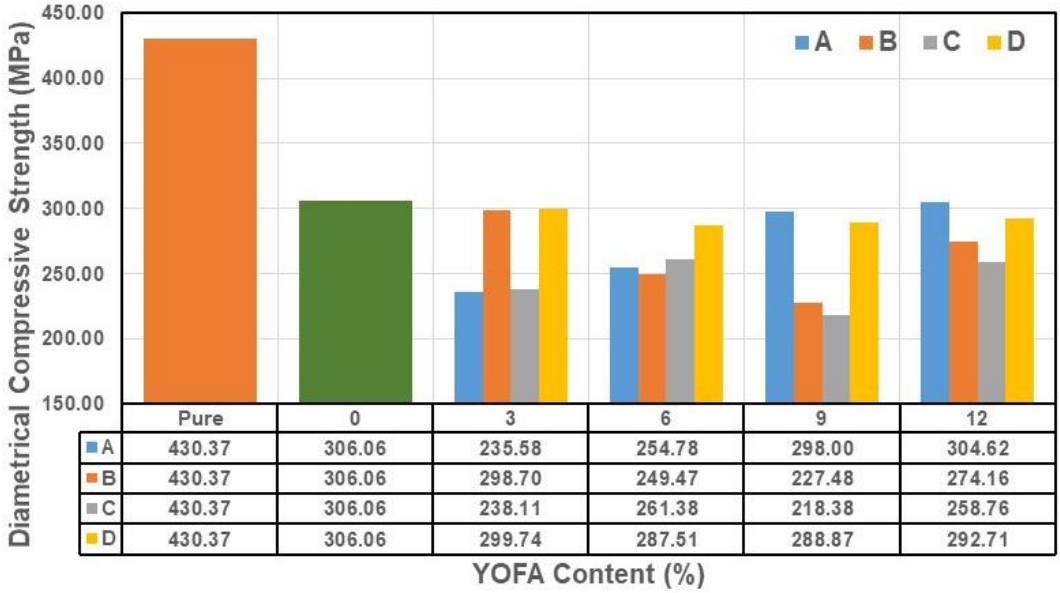
3.2.Hardness and Compressive Strength

Figure 5 depicts the effect of YOFA content, particle size, and graphite on the hardness of the copper composite. Solid copper was the hardest sample investigated in the present study. Adding 3 vol.% graphite to the Cu matrix significantly decreased hardness because graphite is inherently soft and has lubricating properties [39]. In comparison, increasing YOFA significantly increased hardness, indicating its role as a reinforcing phase that hinders plastic deformation and strengthens the composite matrix. Hardness increased with YOFA addition. Smaller particles (A) yielded higher hardness at lower YOFA content because the additive particles were dispersed in the matrix and acted as dislocation buffers when loaded [40]. Nevertheless, when the YOFA content was increased to higher percentages, the hardness decreased due to agglomeration. Coarser particles (B and C) show maximum hardness at 9% YOFA, then decrease again at 12% YOFA. This reduction may be explained by reduced bonding strength between the additive and matrix due to increased porosity at this ratio, as illustrated in Fig. 4, suggesting a best YOFA range of 6 to 9% for hardness, depending on particle size. Controlling fly ash content and particle size is key to enhancing the hardness in copper-graphite composites [41]. Figure 6 shows the dependence of compressive strength on YOFA additive content and grain size. As shown above, compressive strength decreases with graphite addition, which can be attributed to the material's fragility. This decrease continued with increasing YOFA content, which can be attributed to the additive's inherent properties and the high porosity it induces. Regarding the effect of grain size, the compressive strength exhibited a fluctuating trend. However, the highest compressive strength values were generally observed at the highest addition ratio (12%) and across all grain sizes [22]. Decreasing microhardness with increasing radial compressive strength exhibited a typical trade-off behavior also reported for MMCs. The hard YOFA particulates effectively impede dislocation motion and thus increase local hardness. However, the platelets' brittleness reduced the composite's overall load-bearing capacity. The difference in elastic modulus between the soft copper matrix and the hard ceramic phase induced stress concentrations at particle-matrix interfaces under compressive loading. These interfacial regions serve as preferred sites for crack nucleation and propagation, reducing the overall compressive strength even though the densification was enhanced. A considerable divergence was observed in the influence of particle size: microhardness increased with finer YOFA particles. However, compressive strength decreased compared with coarser particles; this behavior results from the balance between increased dispersion strengthening and reduced agglomeration sensitivity. Fine particles can also effectively block dislocation motion locally, thus increasing hardness. Nevertheless, as their surface energy is very high, they tend to aggregate into micro-agglomerates. These agglomerates break the continuity of the copper matrix and behave as stress raisers (sites of crack initiation) when the bulk is subjected to compressive loading, compromising the load at which the bulk fails prematurely, whereas coarser particles, being less efficient hardening agents, allow the matrix to be more continuous, having fewer points of stress concentration.



	Pure	0	3	6	9	12
A	37.23	24.52	30.65	28.67	28.17	26.33
B	37.23	24.52	30.76	22.66	32.11	24.01
C	37.23	24.52	31.82	24.25	33.4	25.27
D	37.23	24.52	23.54	24.85	25.05	25.8

Fig. 5 Variation of Measured Microhardness with YOFA Content.



	Pure	0	3	6	9	12
A	430.37	306.06	235.58	254.78	298.00	304.62
B	430.37	306.06	298.70	249.47	227.48	274.16
C	430.37	306.06	238.11	261.38	218.38	258.76
D	430.37	306.06	299.74	287.51	288.87	292.71

Fig. 6 Variation of Measured Compressive Strength with YOFA Content.

3.3.Tribological Properties

Figure 7 shows the main and interactive effects on wear loss of copper-graphite/YOFA composites under various wear conditions, as detailed in Table 4—the size and content of the additive influence the mechanical and tribological properties of these composites. Wear loss testing was performed using the pin-on-disc method at room temperature under different applied loads for a fixed duration of 20 minutes. Wear loss was calculated from the amount of material residue produced, which is inversely related to wear resistance. Initially, the sample surface adheres directly to the disc; however, as shear forces increase, the surface deforms, and particles detach, creating wear debris. This debris acts as an abrasive medium between the friction surfaces, shifting the wear mechanism from two-body to three-body wear.

3.3.1.Effect of YOFA Concentration on Wear Test

Figure 7 shows the wear test results. This observation is confirmed by the scanning electron microscope (SEM), Fig. 8, which shows that pure copper had the least material loss. However, the matrix composite YCo (Cu + 3% graphite without YOFA) suffered more wear, implying that the presence of graphite itself is not enough to resist the applied load, agreeing with earlier reports on copper–fly ash composites where graphite additions were found to be effective in lubricating the composite only when reinforced with further addition [42, 43], with the wear resistance being more greatly affected by YOFA. In particular, 9% YOFA showed the least wear loss and the best performance among the additives (3%, 6%, and 12%), which suffered greater wear

loss due to a combination of balanced structure and reinforcement stability. YOFA has hard ceramic particles, as shown in Table 1, which act as mechanical reinforcements. However, their effectiveness depends strongly on uniform dispersion and good adhesion between the ceramic particles and the copper matrix. At lower additions, i.e., 3% and 6%, the YOFA amount is too small to form a continuous reinforcement network, leading to poor particle distribution and stress-concentration zones that enhance localized wear. At 9% addition, it can be seen that the particles are much more distributed, allowing for a better mechanical interlock between the reinforcement and the matrix, confirmed by scanning electron microscope (SEM) micrographs (Fig. 9). Figure 9 demonstrates the production of a well-bonded protective tribolayer on the corroded substrate. This tribolayer helps sustain the matrix and mitigates microslip, thus improving wear resistance [7]. On the other hand, increasing the YOFA content to 12% caused particle agglomeration and reduced matrix homogeneity, leading to a severe drop in performance. As a result, poor interfacial bonding and brittle regions form, which are likely to break under load. Some clustered particles broke away during the wear test and acted as free abrasives at the interface between the two solid surfaces; the dominant wear mechanism shifted from adhesive or mild abrasive to severe abrasive wear, causing serious material loss. This behavior was confirmed by SEM images, Fig. 10, which exhibited fractured debris and broken particles on the corroded surfaces at 12% [30]. Thus, the success of reinforcing copper composites with YOFA depends on the uniform dispersion and strong interfacial bonding with the matrix. Just beyond the optimum reinforcement ratio, the matrix structure deteriorates and the corrosion mechanism changes, increasing the corrosion rate.

3.3.2.Effect of Applied Loads on Wear Test

A good positive linear relationship between the normal load and wear loss is shown in Fig. 7. The wear increased with load from 5 N to 20 N gradually in all materials, as confirmed by the scanning electron microscope (SEM) images, as shown in Figs. 9 and 10. The least wear loss was found for pure copper and the Cu-3 vol.% graphite composite (YC0), as shown in Table 5. Higher YOFA additions, particularly at 6 vol.% and 12 vol.%, resulted in large increases in wear at higher loads. Such behavior may be explained by detachment of YOFA particles under high contact stresses, generating hard third-body abrasives that enhance wear. Particle size was also critical: fine YOFA particles (<53 μm) enhanced load bearing and surface smoothness, reducing wear. In comparison, coarse particles (125–150 μm) penetrated the surface and caused abrasive and pull-out mechanisms. These results are consistent with previous studies demonstrating the significance of particle hardness, bonding, and morphology on the wear behavior of copper matrix composites [42-45]. In general, the results demonstrated that normal load is a dominant parameter for wear loss, and that its effect is modulated by particle size and the strength of the reinforcement–matrix interface. According to Archard's law [2, 32], wear loss is characterized in terms of the other parameters, with the prediction that wear loss is inversely proportional to the hardness of the composite, as expressed in Eq. (5):

$$L = K\frac{NG}{CH} \quad (5)$$

where L, H, G, N, K, and C represent the amount of wear, material hardness, sliding distance, applied normal load, the wear constant, and the geometrical microstructure factor, respectively. Therefore, the wear resistance based on hardness in Archard's wear law reduces particle contact force, increasing the chance of severe contact between tribosurfaces. Additionally, asperity junctions from stick-slip allow wear debris to form at smaller YOFA particle sizes. Furthermore, the third-body mechanism may increase abrasive action if YOFA wear debris remains trapped at the sliding interface. The rubbing of soft, worn debris from the matrix phase can also cause the secondary layer to break apart. All of these processes intensify as YOFA particle size increases, causing further material de-bonding and dislodging from the primary surfaces.

Table 5 Designation and Composition of Reinforced Copper Composites

Property	Pure	YC0	YC3	YC6	YC9	YC12
Composition	Pure copper (100% Cu)	97% Cu + 3% Gr	94% Cu + 3% Gr + 3%YOFA	91% Cu + 3% Gr + 6%YOFA	88% Cu + 3% Gr + 9%YOFA	85% Cu + 3% Gr +12% YOFA

3.3.3.Effect of Particle Size on Wear Test

Adding YOFA particles with graphite showed a clear effect of particle size. The reinforced composites YC3, YC6, YC9, and YC12, containing 3%, 6%, 9%, and 12% YOFA, respectively, and 3% graphite, as tabulated in Table 5, exhibited a clear particle-size dependence. The main effects plot shows a wear loss increasing with particle size. Fine particles (<53 μm) enhanced the dispersion in the copper–graphite matrix and promoted the formation of a stable tribological film, resulting in large decreases in wear. Chew et al. [43] and Balamurugan and Uthayakumar [44] reported similar results, confirmed by scanning electron microscope (SEM) images, Fig. 9. The

densification is promoted, and porosity is decreased. The mechanical and wear properties are improved by the fine fly ash reinforcements. In contrast, coarse particles (125–150 μm) had an abrasive effect by enhancing micro-cutting and plowing; hence, wear increased, which agrees with the findings of Sai et al. [42] and Balamurugan and Uthayakumar [45]. In addition, load affected wear more significantly than particle size and reinforcement content. Wear loss increased drastically as the load increased; this trend was also reported in other tribological studies [44]. The results indicated that the wear resistance can be effectively improved by fine YOFA particles. Protectiveness decreased as particle size increased; thus, particle size is critical for optimizing the tribological performance of Cu–Gr–YOFA composites. This improvement was attributed to the enhanced dispersion of fine particles in the copper–graphite matrix that favors the formation of a stable protective friction layer (tribolayer). By contrast, coarse particles tended to behave abrasively because particle (debris) detachment increased fine cutting and plowing on the sliding surface.

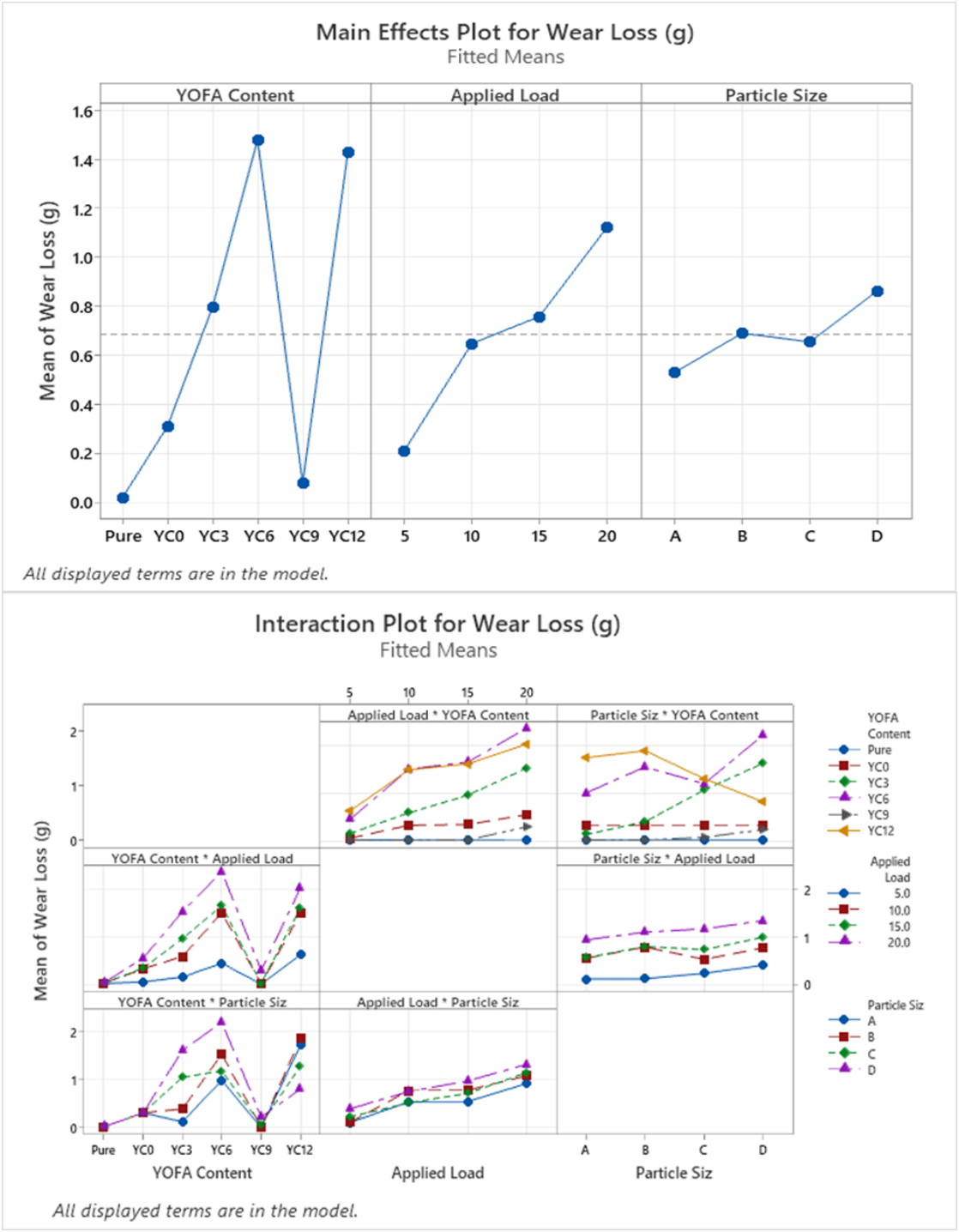


Fig. 7 Effect of YOFA Content, Applied Loads, and Particle Size on Wear Test.

3.3.4.Full-Factorial Design of the Experiment

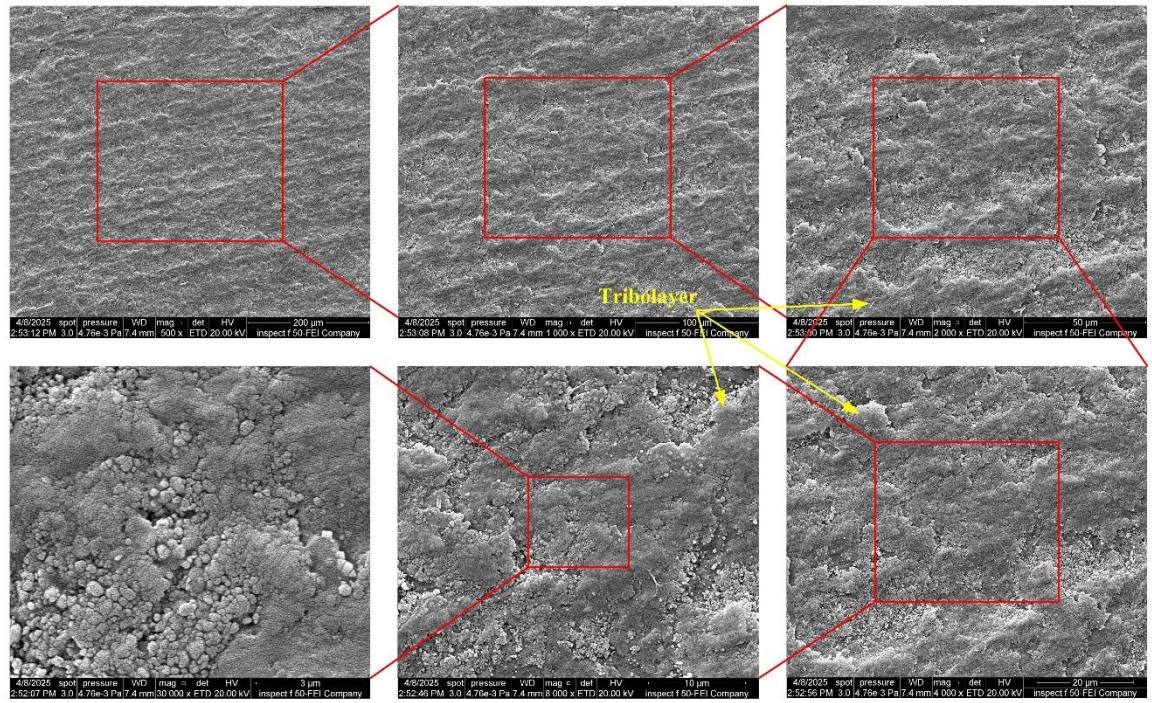
One statistical method to assess the separate effects of control factors is ANOVA. ANOVA is also a numerical design tool that separates the effect of each control factor. To determine each factor's effect on the quality characteristic, it computes the percentage contribution [38, 46]. The results of the ANOVA analysis are summarized in Table 6 with a 95% confidence level (P-value) of 0.5%. The values in the fifth column of these tables are "Adj SS," or Adjusted Sum of Squares, computing the percentage of variability of the dependent variable that can be explained by the changes in independent variables. In ANOVA, the F-statistic follows an F-distribution (assuming the null hypothesis is true) and is used to obtain a p-value to determine significance. The "F value" is the mean square error variance divided by the mean square factor variance. The P-value, when the null hypothesis H0 is true, is the probability that the test statistic is as extreme as or more extreme than the observed value [46]. The composite performs' P-values and error contributions are all close to zero, suggesting that the factors have a major impact on wear rate and wear loss. The influence of controllable elements is indicated by the degrees of freedom (DF) [46]. Because the experimental design used only replication for three factors—YOFA composition, particle size, and applied force—and one response—wear loss—the ANOVA table shows an error sum of squares of zero. Because there is only one replication, the degrees of freedom are 0 when the error mean square and error sum of squares are also zero. As a result, the F0 value stays at zero. According to the R-squared value, the model accounts for roughly 100% of wear loss. Strong significance is indicated by a high coefficient of determination (R-squared), which gauges how well the model fits the data [47]. The chosen control parameters and their interactions are statistically and physically significant for the wear loss of the composites, as indicated by the ANOVA table's lack of residual error. Their interaction contributions also outweigh the error. The parameters that most influence the output response are also highlighted in the contribution column. It demonstrates that the primary determinants of wear loss are YOFA content and applied load, with smaller impacts from particle size, and two-way and three-way interactions. Surprisingly, the wear behavior of the composites was predominantly governed by the YOFA content and the applied stress rather than any other variables or interactions. At a 95% confidence level, the three-way interaction effect was insignificant, suggesting no residual error. In addition to the control factors, uncontrollable factors such as machine vibrations, environmental conditions, and pin and disc surface finish also impacted the response values. The viscoelastic and temperature-related characteristics of metals and metal matrix composites significantly impacted their tribological behavior. Interface temperature rose because heat was generated at contact locations during sliding. The material's viscoelastic characteristics, including stress response, adhesion, and transfer behaviors, were impacted by this temperature increase. Extended sliding further raises the friction surface temperature, which can seriously impair the composites' mechanical properties and cause material loss [38]. As a result, YOFA content and applied load influence wear characteristics more than any other factor or combination of factors.

Table 6 ANOVA Results for Wear Loss.

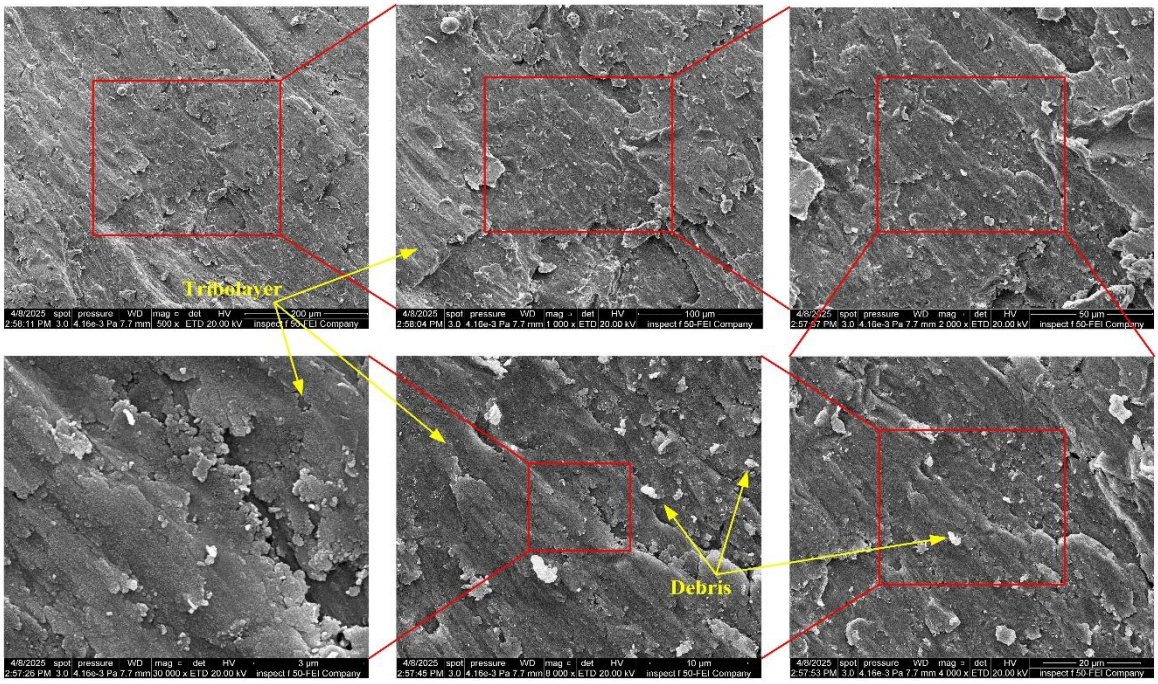
	DF	Seq SS	Contribution	Adj SS	Adj MS	F-Value	P-Value
Model	95	67.3669	100.00%	67.3669	0.70913	*	*
Linear	11	45.7954	67.98%	45.7954	4.16321	*	*
YOFA Content	5	34.2854	50.89%	34.2854	6.85708	*	*
Applied Load	3	10.1509	15.07%	10.1509	3.38364	*	*
Particle Size	3	1.3590	2.02%	1.3590	0.45301	*	*
2-Way Interactions	39	16.9062	25.10%	16.9062	0.43349	*	*
YOFA Content*Applied Load	15	6.2145	9.22%	6.2145	0.41430	*	*
YOFA Content*Particle Size	15	10.3292	15.33%	10.3292	0.68862	*	*
Applied Load*Particle Size	9	0.3625	0.54%	0.3625	0.04028	*	*
3-Way Interactions	45	4.6654	6.93%	4.6654	0.10367	*	*
YOFA Content*Applied Load*Particle Size	45	4.6654	6.93%	4.6654	0.10367	*	*
Error	0	*	*	*	*		
Total	95	67.3669	100.00%				

Model Summary

S	R-sq	R-sq(adj)	PRESS	R-sq(pred)	AICc	BIC
*	100.00%	*	*	*	*	*

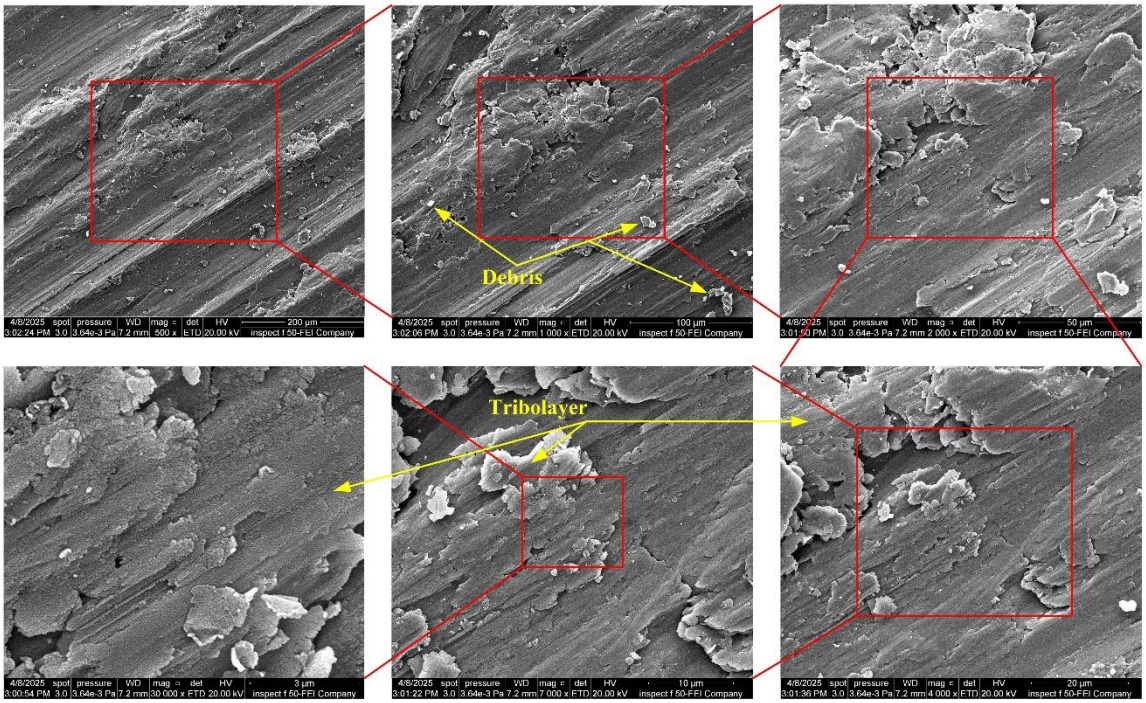


(a)

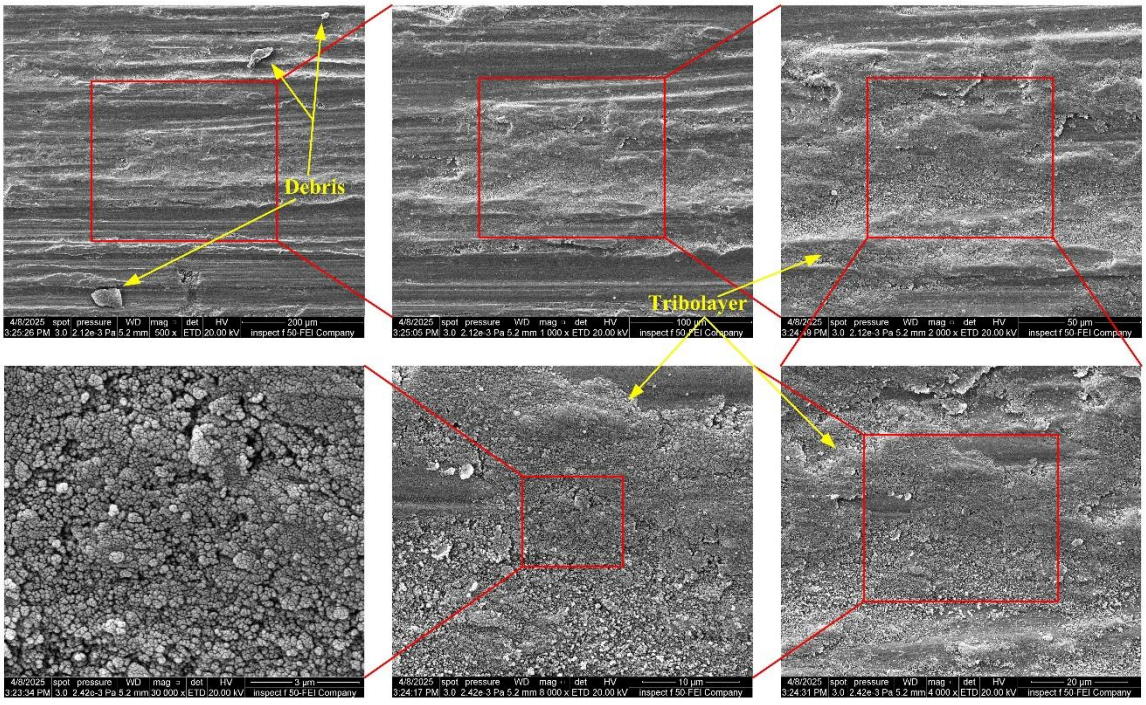


(b)

Fig. 8 Worn Surface Analysis of Copper Matrix Composites: (a) Pure Copper (Cu) and (b) Pure Copper (Cu) + 3% Gr.

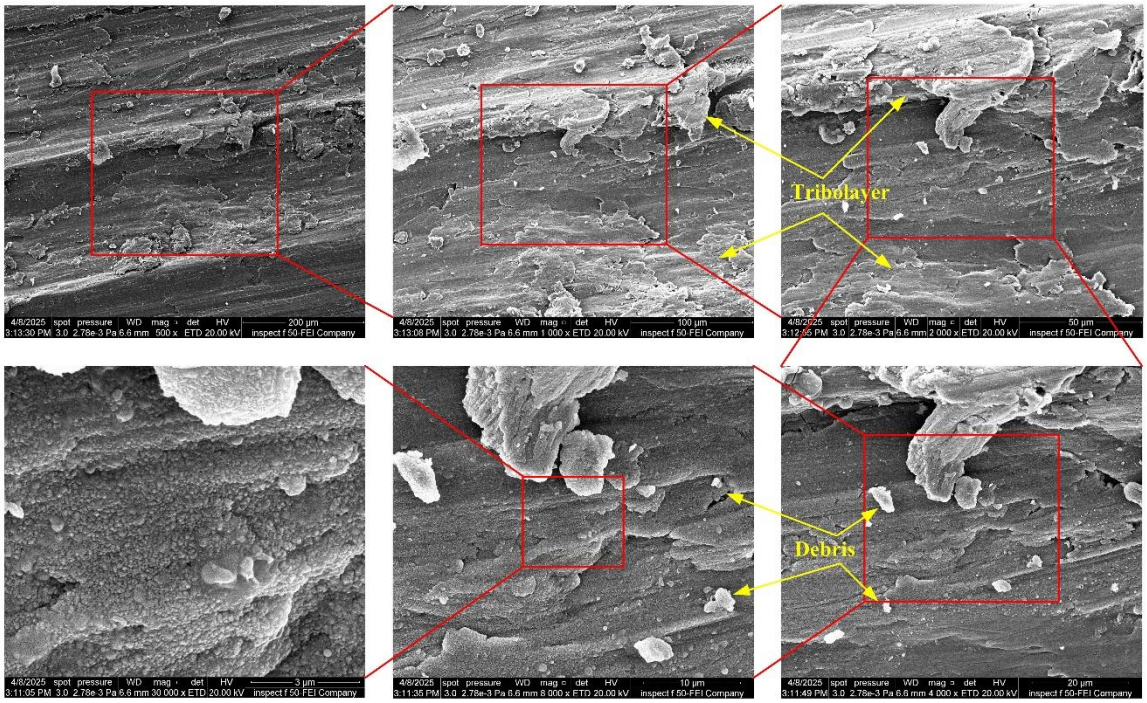


(a)

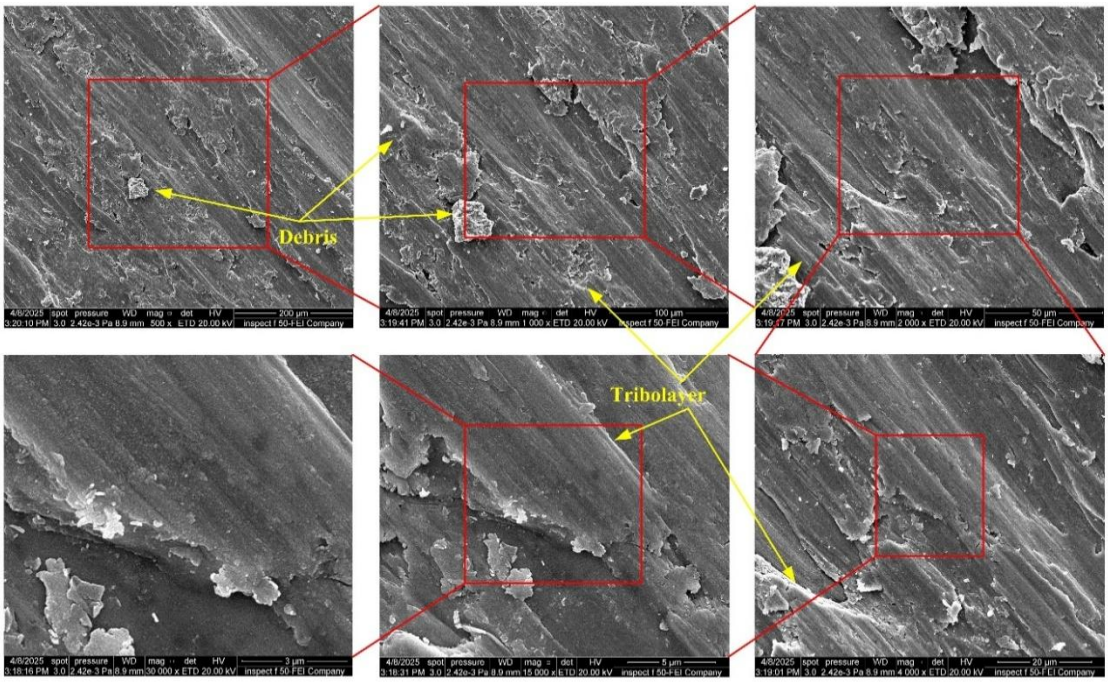


(b)

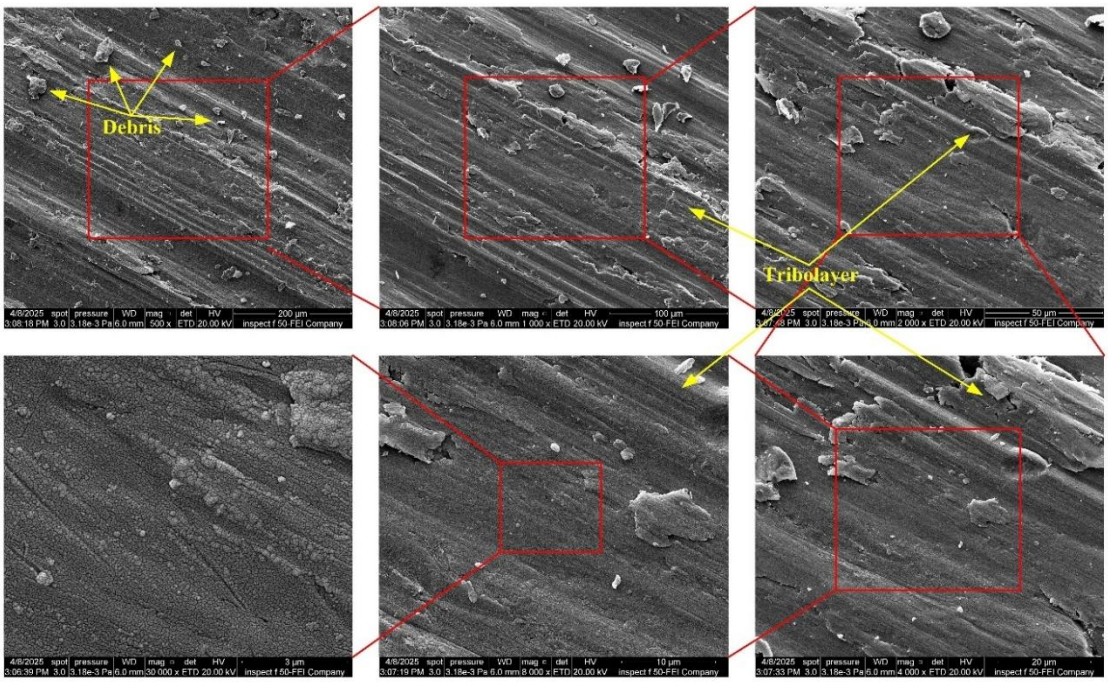
Fig. 9 Worn Surface Analysis of Copper Matrix Composites
(a) Cu+3%Gr+9% YOFA (53 µm) at 5 N (b) Cu+3%Gr+9% YOFA (125 -150) µm at 5N.



(a)



(b)



(c)

Fig. 10 Worn Surface Analysis of Copper Matrix Composites (a) Cu+3%Gr+9% YOFA (125-150) µm at 20 N (Cu) (b) Cu+3%Gr+12% YOFA (53) µm at 20 N (c) Cu+3%Gr+12% YOFA (125-150) µm at 20 N.

4.CONCLUSIONS

The present work investigated the impact of YOFA on the physical, mechanical, and tribological properties of copper–graphite composites. The key results are listed below:

1- Increasing the proportion of YOFA reduced the total density of the composites, whereas fine YOFA particles (<53 µm) decreased porosity and improved the structural integrity of the composites.
2- The hardness of pure copper decreased with the addition of crude graphite, followed by improved microhardness with YOFA reinforcement; the best results were at 6–9 vol.% YOFA, depending on particle size.
3- Generally, radial compressive strength decreased with graphite and YOFA additives; however, a significant increase was observed at 12 vol.% YOFA.
4- Wheel-on-disk tests showed that 9 vol.% YOFA with fine particles provided the highest wear resistance due to homogeneous particle dispersion and the formation of a protective tribolayer.
5- High YOFA content (12 vol.%) and larger particle sizes induced particle agglomeration, weak bonding, and abrasive wear, leading to inferior performance.
6- YOFA was a promising sustainable reinforcement, and fine particles at ~9 vol.% offered the best trade-off of hardness, strength, and tribological stability for future use in the electrical and automotive sectors.
7- ANOVA results indicated that YOFA content was the dominant factor, accounting for 50.9% of the variance, confirming its importance in determining the material behavior. The applied load contributed about 15.1% of the total, indicating its mechanical significance. Particle size also had a small direct effect of 2.0%, mainly indirectly through interactions. The next largest two-way interaction effect was YOFA content × particle size (15.3%), followed by YOFA content × applied load (9.2%). In contrast, the applied load × particle size interaction was insignificant. The three-factor interaction added 6.9%, indicating synergy. In sum, these results emphasize that optimal material performance depends on the coupled control of composition, load conditions, and particle size.

REFERENCES

[1] Annaz AA, Irhayyim SS, Hamada ML, Hammood HS. **Comparative Study of Mechanical Performance Between Al-Graphite and Cu-Graphite Self-Lubricating Composites Reinforced by Nano-Ag Particles**. *AIMS Materials Science* 2020; 7(5): 534–551.

[2] Mahdi FM, Razooqi RN, Irhayyim SS. **The Influence of the Graphite Content and Milling Time on the Hardness, Compressive Strength and Wear Volume of Copper - Graphite Composites Prepared Via Powder Metallurgy**. *Tikrit Journal of*

Engineering Sciences 2017; **24**(3): 38–44.

[3] Irhayyim SS, Hammood HS, Meteab MM. **Gravel Powder Effect in Reinforced Aluminum Alloy Matrix Composite**. *Materials Today: Proceedings* 2020; **20**: 548–554.

[4] Deng Z, Zhou X, Zhang J, Li Y, Wang H, Chen X, Liu Y. **Microstructure and Mechanical Properties of Cu–12Al–xNi Alloy Prepared Using Powder Metallurgy**. *Materials Science and Engineering: A* 2019; **759**: 241–251.

[5] Meignanamoorthy M, Ravichandran M. **Synthesis of Metal Matrix Composites Via Powder Metallurgy Route**. *Mechanics and Mechanical Engineering* 2018; **22**(1): 59–69.

[6] Surekha K, Els-Botes A. **Development of High Strength, High Conductivity Copper by Friction Stir Processing**. *Materials & Design* 2011; **32**(2): 911–916.

[7] Narayanasamy P, Balaji AN, Vettivel SC. **Microstructural, Electrical, Thermal, and Tribological Studies of Copper-Fly Ash Composites Through Powder Metallurgy**. *Bulletin of the Polish Academy of Sciences: Technical Sciences* 2018; **66**(6): 935–940.

[8] Guo MX, Shen K, Wang MP. **Effect of In Situ Reaction Conditions on the Microstructure Changes of Cu–TiB2 Alloys by Combining in Situ Reaction and Rapid Solidification**. *Materials Chemistry and Physics* 2012; **131**(3): 589–599.

[9] Mun YS, Jo JH, Park GD, Kang YC. **Copper–Antimony–Red Phosphorus Composites as Promising Anode Materials for Sodium-Ion Batteries**. *Journal of Power Sources* 2017; **362**: 115–122.

[10] Ahn BW, Kim JH, Hamad K, Jung SB. **Microstructure and Mechanical Properties of a B4C Particle-Reinforced Cu Matrix Composite Fabricated by Friction Stir Welding**. *Journal of Alloys and Compounds* 2017; **693**: 688–691.

[11] Irhayyim SS. **Effect of Graphite/WC Additions on Physical, Mechanical, and Wear Properties of Aluminum**. *Diyala Journal of Engineering Sciences* 2017; **10**(1): 72–86.

[12] Razooqi RN, Razej KH, Abdulhameed AT, Irhayyim SS. **The Physical and Mechanical Properties of a Shape Memory Alloy Reinforced with Carbon Nanotubes (CNTs)**. *Tikrit Journal of Pure Science* 2018; **23**(9): 80–88.

[13] Liu Q, Castillo-Rodríguez M, Galisteo AJ, Guzmán de Villoria R, Torralba JM. **Wear Behavior of Copper–Graphite Composites Processed by Field-Assisted Hot Pressing**. *Journal of Composites Science* 2019; **3**(1): 29.

[14] Mahdi AD, Irhayyim SS, Abduljabbar SF. **Mechanical and Wear Behavior of Al7075-Graphite Self-Lubricating Composite Reinforced by Nano-WO3 Particles**. *Materials Science Forum* 2020; **1002**: 151–160.

[15] Chen K, Zhang L, Xie T, Wei X. **Study on Graphite Motion Law of Copper-Based Graphite Composites During Friction**. *Journal of Advanced Mechanical Design, Systems, and Manufacturing* 2024; **18**(3): 2024jamdsm0026.

[16] Rajesh R, Balaji AN, Narayanasamy P, Vettivel SC. **Study on Conventional and Microwave-Assisted Sintering of Cu-FA Composites**. *Materials Today: Proceedings* 2021; **39**: 1677–1681.

[17] Dinaharan I, Albert T. **Effect of Reinforcement Type on Microstructural Evolution and Wear Performance of Copper Matrix Composites Via Powder Metallurgy**. *Materials Today Communications* 2023; **34**: 105250.

[18] da Motta CAO, dos Santos CA, Garcia A, Spim JA. **Enhancing Composite Materials Through Fly Ash Reinforcement Through Powder Metallurgy**. *Materials Chemistry and Physics* 2023; **307**: 128124.

[19] Zou H, Ran X, Zhu W, Wang Y, Zhan S, Hao Z. **Tribological Behavior of Copper–Graphite Composites Reinforced with Cu-Coated or Uncoated SiO2 Particles**. *Materials* 2018; **11**(12): 2414.

[20] Dinaharan I, Albert T, David Raja Selvam J. **Microstructure and Wear Performance of Fly Ash-Reinforced Copper Matrix Composites Prepared Via Powder Metallurgy**. *Journal of Materials Engineering and Performance* 2024; **33**(24): 14161–14176.

[21] Balamurugan P, Uthayakumar M, Niemczewska-Wójcik M. **Wear Studies of Copper-Fly Ash Composite Under Dry Sliding Conditions**. *Materials Research Express* 2019; **6**(10): 1065d5.

[22] Rajan STK, Balaji AN, Raghav GR, Vettivel SC. **Compression and Corrosion Behaviour of Sintered Copper-Fly Ash Composite Material**. *Materials Research Express* 2019; **6**(4): 046524.

[23] **Influence of Concentration and Particle Size of Yellow Oil Fly Ash on Thermal and Mechanical Properties of High-Density Polyethylene**. *Jordan Journal of Mechanical and Industrial Engineering* 2025; **19**(1): 129–146.

[24] ASTM B962-08. **Standard Test Methods for Density of Compacted or Sintered Powder Metallurgy (PM) Products Using Archimedes' Principle**. ASTM International, West Conshohocken, PA; 2008.

[25] Horath L. **Fundamentals of Materials Science for Technologists: Properties, Testing, and Laboratory Exercises**. 3rd ed., Waveland Press, Inc.; 2019.

[26] Huang SJ, Abbas A, Ballóková B. **Effect of CNT on Microstructure, Dry Sliding Wear and Compressive Mechanical Properties of AZ61 Magnesium Alloy**. *Journal of Materials Research and Technology* 2019; **8**(5): 4273–4286.

[27] Zeng F, Dong X, Wang Q, Zhang C, Wu Y, Ding W. **Fabrication and Mechanical Properties of Mesoporous Silica Nanoparticles Reinforced Magnesium Matrix Composite**. *Journal of Alloys and Compounds* 2017; **728**: 413–423.

[28] AlGharagoly HSH. **Effect of Pressing Pressure on Properties of Copper–10% Graphite Composites Prepared by Powder Metallurgy Technique**. *Tikrit Journal of Engineering Sciences* 2016; **24**(2): 28–34.

[29] ASTM E384-22. **Standard Test Method for Microindentation Hardness of Materials**. ASTM International, West Conshohocken, PA; 2022.

[30] Irhayyim SS, Hammood HS, Mahdi AD. **Mechanical and Wear Properties of Hybrid Aluminum Matrix Composite Reinforced with Graphite and Nano MgO Particles Prepared by Powder Metallurgy Technique**. *AIMS Materials Science* 2020; **7**(1): 103–115.

[31] Irhayyim SS, Hammood HS, Abdulhadi HA. **Effect of Nano-TiO2 Particles on Mechanical Performance of Al–CNT Matrix Composite**. *AIMS Materials Science* 2019; **6**(6): 1124–1134.

[32] Irhayyim SS, Ahmed SR, Annaz AA. **Mechanical Performance of Micro-Cu and Nano-Ag Reinforced Al-CNT Composite Prepared by Powder Metallurgy Technique**. *Materials Research Express* 2019; **6**(10): 105071.

[33] ASTM G99-95a. **Standard Test Method for Wear Testing with a Pin-on-Disk Apparatus**. ASTM International, West Conshohocken, PA; 2017.

[34] Hammood HS, Mahmood AS, Irhayyim SS. **Effect of Graphite Particles on Physical and Mechanical Properties of Nickel Matrix Composite**. *Periodicals of Engineering and Natural Sciences* 2019; **7**(3): 1318–1328.

[35] Xiao Y, Zhang Z, Yao C, Wang Y, Kadochkin A, Zhang Y. **Investigation on Speed-Load Sensitivity to Tribological Properties of Copper Metal Matrix Composites for Braking Application**. *Metals* 2020; **10**(7): 889.

[36] Ning H, Wang Z, Zhao X, Liu Y, Zhang S, Lu Y. **Modeling and Prediction of Tribological Properties of Copper/Aluminum-Graphite Self-Lubricating Composites Using Machine Learning Algorithms**. *Friction* 2024; **12**(6): 1322–1340.

[37] Radhika N, Sam M. **Tribological and Wear Performance of Centrifuge Cast Functional Graded Copper-Based Composite at Dry Sliding Conditions**. *Journal of Central South University* 2019; **26**(11): 2961–2973.

[38] Balamurugan P, Uthayakumar M. **Influence Study of Manufacturing Constraints and Percentage of Reinforcement on Copper-Fly Ash Composite by Full Factorial Design**. *International Journal of Computer Aided Engineering and Technology* 2018; **10**(6): 673–683.

[39] Li H, Zhang Z, Dong C, Wu G, Yang H. **On the Tribological Behaviors of Cu Matrix Composites with Different Cu-Coated Graphite Content**. *Journal of Materials Research and Technology* 2023; **25**: 83–94.

[40] Santhosh MS, Sasikumar C, Natarajan E, Kumar RS. **Mechanical and Wear Behaviour of Nano-Fly Ash Particle-Reinforced Mg Metal Matrix Composites Fabricated by Stir**

Casting Technique. *Journal of Nanomaterials* 2022; **2022**: 5465771.

[41] Shankar KV, Sharma S, Verma A. **Investigating the Effect of Fly Ash Addition on the Metallurgical and Mechanical Behavior of Al-Si-Mg-Cu Alloy for Engine Cylinder Head Application**. *Materials* 2022; **15**(15): 5462.

[42] Sai NV, Komaraiah M, Raju AVSR. **Preparation and Properties of Sintered Copper–Tin Composites Containing Copper Coated or Uncoated Fly Ash**. *Materials and Manufacturing Processes* 2008; **23**(7): 651–657.

[43] Chew PY, Zahi S, You AH, Lim PS, Ng MC. **Preparation of Cu and Fly Ash Composite by Powder Metallurgy Technique**. *AIP Conference Proceedings* 2011; **1328**(1): 208–210.

[44] Balamurugan P, Uthayakumar M. **Influence of Process Parameters on Cu–Fly Ash Composite by Powder Metallurgy Technique**. *Materials and Manufacturing Processes* 2015; **30**(3): 313–319.

[45] Balamurugan P, Uthayakumar M. **Wear Studies on SiC and Fly Ash Reinforced Copper Based Composites by Grey Relational Analysis**. *Advanced Materials Research* 2014; **984-985**: 304–312.

[46] Haiter Lenin A, Vettivel SC, Raja T, Belay L, Singh SCE. **A Statistical Prediction on Wear and Friction Behavior of ZrC Nano Particles Reinforced with Al Si Composites Using Full Factorial Design**. *Surfaces and Interfaces* 2018; **10**: 149–161.

[47] Gangatharan K, Selvakumar N. **Optimizing the Dry Sliding Wear Behavior of Copper Hybrid Nano Composites Reinforced with MWCNTs and Nano B4C Using Full Factorial Design**. *Transactions of the Indian Institute of Metals* 2016; **69**(3): 717–732.